Mathematical and Computational Applications

MDPI

Article

A Numerical Method Based on Operator Splitting Collocation Scheme for Nonlinear Schrödinger Equation

Mengli Yao and Zhifeng Weng *

Fujian Province University Key Laboratory of Computation Science, School of Mathematical Sciences, Huaqiao University, Quanzhou 362021, China; yaomengli163@163.com
* Correspondence: zfwmath@163.com

Abstract: In this paper, a second-order operator splitting method combined with the barycentric Lagrange interpolation collocation method is proposed for the nonlinear Schrödinger equation. The equation is split into linear and nonlinear parts: the linear part is solved by the barycentric Lagrange interpolation collocation method in space combined with the Crank–Nicolson scheme in time; the nonlinear part is solved analytically due to the availability of a closed-form solution, which avoids solving the nonlinear algebraic equation. Moreover, the consistency of the fully discretized scheme for the linear subproblem and error estimates of the operator splitting scheme are provided. The proposed numerical scheme is of spectral accuracy in space and of second-order accuracy in time, which greatly improves the computational efficiency. Numerical experiments are presented to confirm the accuracy, mass and energy conservation of the proposed method.

Keywords: nonlinear Schrödinger equation; operator splitting collocation method; barycentric Lagrange interpolation; consistency analysis; convergence analysis

check for updates

Citation: Yao, M.; Weng, Z. A Numerical Method Based on Operator Splitting Collocation Scheme for Nonlinear Schrödinger Equation. *Math. Comput. Appl.* **2024**, *29*, 6. https://doi.org/10.3390/mca29010006

Academic Editor: Sundeep Singh

Received: 19 November 2023
Revised: 27 December 2023
Accepted: 12 January 2024
Published: 15 January 2024

1. Introduction

In 1926, the famous Schrödinger equation was proposed by the Austrian physicist Schrödinger [1]. It's a fundamental equation in the field of quantum mechanics. In recent years, the Schrödinger equation has been studied in different fields of research, such as atomic, molecular, nuclear physics and solid state physics, etc.

In this paper, we consider the following nonlinear Schrödinger (NLS) equation

$$\begin{cases} iu_t + \rho\Delta u + v(\mathbf{x})u + \beta|u|^2 u = 0, (\mathbf{x}, \mathrm{t}) \in \Omega \times (0, \mathrm{T}] \\ u(\mathbf{x}, 0) = u_0(\mathbf{x}), \mathbf{x} \in \Omega \\ u(\mathbf{x}, t) = 0, \mathbf{x} \in \partial\Omega, \mathrm{t} \in (0, \mathrm{T}] \end{cases}, \tag{1}$$

where i is the imaginary unit, ρ, β are real-valued constants, $\Omega \subset R^d (d = 1, 2)$ is a bounded area and Δ is the Laplace operator. The function $u_0(\mathbf{x})$ is a given sufficiently smooth function and $v(\mathbf{x})$ is a real-valued potential function. This model reflects the quantum mechanical effects and microscopic system properties and can well describe the state of microscopic particles over time.

In fact, the NLS Equation (1) also conserves both mass and energy with the following mass and energy functions:

$$M(t) = \int_\Omega |u(\mathbf{x}, t)|^2 d\mathbf{x} = M(0) \tag{2}$$

and

$$E(t) = \int_\Omega (\rho|\nabla u(\mathbf{x}, t)|^2 - v(\mathbf{x})|u(\mathbf{x}, t)|^2 - \frac{\beta}{2}|u(\mathbf{x}, t)|^4) d\mathbf{x} = E(0). \tag{3}$$

Recently, many numerical methods have been developed for solving the NLS equation. Gong et al. [2] presented a conservative Fourier pseudo-spectral method for the nonlinear

Schrödinger equation. Cui et al. [3] developed mass- and energy-preserving exponential Runge–Kutta methods for the nonlinear Schrödinger equation. Feng et al. [4] developed the high-order mass- and energy-conserving SAV-Gauss collocation finite element methods for the NLS equation. Wang et al. [5] used the two-grid finite element method for the NLS equation and the given superconvergence analysis of the scheme. Wang et al. [6] studied leapfrog finite element methods for a class of nonlinear Schrödinger equations with damped terms. Hu et al. [7] presented the Newton iterative Crank–Nicolson finite element method for the NLS equation. Chen et al. [8] applied the two-grid finite volume element method for the time-dependent Schrödinger equation. Deng et al. [9] considered a second-order SAV scheme for the nonlinear Schrödinger equation in the whole space with typical generalized nonlinearities and carried out a rigorous error analysis. Su et al. [10] considered the numerical solution of the nonlinear Schrödinger equation with a highly oscillatory potential (NLSE-OP) and rigorously analyzed the error bounds of the splitting schemes for solving the NLSE-OP to a fixed time. Wang et al. [11] proposed finite difference methods for the coupled Gross–Pitaevskii equations in high dimensions and the given error estimates.

There are some advantages, such as no dividing elements, simple formulas, no integrals and easy programming, of the collocation method, which is called the barycentric Lagrange interpolation collocation (BLIC) method. The method has captured the attention of many scholars because of its high accuracy. The numerical stability of the barycentric Lagrange interpolation collocation method with Chebyshev points is very good, and it can also effectively overcome the "Runge" phenomenon. The method has been extended to solve various partial differential equations, such as the sine-Gordon equation [12], the Burgers equation [13], the viscoelastic wave equation [14], the Allen–Cahn equation [15,16], nonlinear convection-diffusion optimal control problems [17] and the fractional telegraph equation [18], among others.

To the best of our knowledge, there are few studies regarding using the barycentric interpolation collocation method combined with the operator splitting method [19–21] for the nonlinear Schrödinger equation. Based on the above work, we focus on the convergence analysis of the proposed scheme. We analyze the fully discretized consistency of the linear subproblem. Moreover, the error estimates of the operator splitting scheme are derived.

The remaining parts of the paper are structured as follows. In Section 2, we present the barycentric Lagrange interpolation collocation method. In Section 3, we present a second-order operator splitting collocation scheme for the NLS equation. The convergence analyses of the proposed method are presented in Section 4. Numerical experiments are conducted in Section 5 to evaluate the accuracy and efficiency of the proposed method, while Section 6 presents some conclusions derived from these experiments.

2. Preliminary

Suppose that $m+1$ distinct interpolation nodes, x_j $(j=0,1,\ldots,m)$, and their corresponding function values, u_j, are provided. Therefore, there exists a unique interpolation polynomial whose degree is not exceeding m, satisfying $q(x_j)=u_j$ $(j=0,1,\ldots,m)$. As we know, $q(x)$ has the Lagrange form as follows,

$$q(x)=\sum_{j=0}^{m} G_j(x)u_j, \tag{4}$$

where $G_j(x)$ represents the Lagrange interpolation basis function and

$$G_j(x)=\frac{\prod\limits_{i=0,i\neq j}^{m}(x-x_i)}{\prod\limits_{i=0,i\neq j}^{m}(x_j-x_i)}, \quad j=0,1,\cdots,m. \tag{5}$$

Suppose that

$$g(x) = (x - x_0)(x - x_1)\dots(x - x_m), \tag{6}$$

and the barycentric weights are defined as follows:

$$w_j = \frac{1}{\prod\limits_{i=0, i\neq j}^{m}(x_j - x_i)}, \quad j = 0, 1, \cdots, m. \tag{7}$$

Then, from Equations (5)–(7), we can obtain

$$G_j(x) = g(x)\frac{w_j}{x - x_j}, \quad j = 0, 1, \cdots, m. \tag{8}$$

By Equations (8) and (4), we have

$$q(x) = g(x)\sum_{j=0}^{m}\frac{w_j}{x - x_j}u_j. \tag{9}$$

If $u = 1$, it has the following form:

$$1 = g(x)\sum_{j=0}^{m}\frac{w_j}{x - x_j}. \tag{10}$$

By Equations (10) and (9), the barycentric interpolation formula of $q(x)$ can be derived:

$$q(x) = \frac{\sum\limits_{j=0}^{m}\frac{w_j}{x - x_j}u_j}{\sum\limits_{j=0}^{m}\frac{w_j}{x - x_j}} = \sum_{j=0}^{m}\frac{\frac{w_j}{x - x_j}}{\sum\limits_{j=0}^{m}\frac{w_j}{x - x_j}}u_j := \sum_{j=0}^{m}\tilde{G}_j(x)u_j. \tag{11}$$

To ensure the numerical stability of the barycentric Lagrange interpolation, we adopt Chebyshev points:

$$x_j = cos(\frac{j}{m}\pi), j = 0, 1, \cdots, m. \tag{12}$$

The v-order derivative of $q(x)$ defined as Equation (11) with respect to x is

$$q^{(v)}(x_i) = \frac{d^v q(x_i)}{dx^v} = \sum_{j=0}^{m}\tilde{G}_j^{(v)}(x_i)u_j = \sum_{j=0}^{m}P_{ij}^{(v)}u_j, v = 1, 2, \cdots, m, \tag{13}$$

where $P_{ij}^{(v)}$ denotes the element of the v-order differentiation matrix $P^{(v)}$.

From Equations (11) and (13), we can obtain [22]

$$\begin{cases} P_{ij}^{(1)} = \tilde{G}_j'(x_i) = \frac{w_j/w_i}{x_i - x_j}, j \neq i, \\ P_{ii}^{(1)} = -\sum\limits_{j=0, j\neq i}^{m}P_{ij}^{(1)}, \end{cases} \tag{14}$$

$$\begin{cases} P_{ij}^{(2)} = \tilde{G}_j''(x_i) = -2\frac{w_j/w_i}{x_i - x_j}\left(\sum\limits_{k\neq i}\frac{w_k/w_i}{x_i - x_k} + \frac{1}{x_i - x_j}\right), j \neq i, \\ P_{ii}^{(2)} = -\sum\limits_{j=0, j\neq i}^{m}P_{ij}^{(2)}. \end{cases} \tag{15}$$

Next, we will derive the approximation format for a given function, $u(x,y)$, and its derivative using the barycentric Lagrange interpolation formula.

For $m+1$ distinct nodes, $(x_0,y),(x_1,y),\ldots,(x_m,y)$, the unknown function $u(x,y)$, evaluated at node (x_i,y), can be expressed as follows:

$$u(x_i,y), \quad i=0,1,\ldots,m. \tag{16}$$

From Equations (16) and (11), we can obtain the approximation function of $u(x,y)$:

$$u(x,y)=\sum_{i=0}^{m}\alpha_i(x)u(x_i,y), \quad i=0,1,\ldots,m. \tag{17}$$

Similarly, the expression of $u(x_i,y)$ is as follows:

$$u(x_i,y)=\sum_{j=0}^{n}\beta_j(y)u(x_i,y_j), \quad j=0,1,\ldots,n. \tag{18}$$

From Equations (17) and (18), we can obtain

$$u(x,y)=\sum_{i=0}^{m}\sum_{j=0}^{n}\alpha_i(x)\beta_j(y)u(x_i,y_j), \tag{19}$$

and its second-order partial derivative has the following form:

$$u_{xx}(x,y)=\sum_{i=0}^{m}\sum_{j=0}^{n}\alpha_i''(x)\beta_j(y)u(x_i,y_j), \tag{20}$$

$$u_{yy}(x,y)=\sum_{i=0}^{m}\sum_{j=0}^{n}\alpha_i(x)\beta_j''(y)u(x_i,y_j). \tag{21}$$

3. Operator Splitting Collocation Method

In this section, we propose an operator splitting collocation scheme for the NLS equation, which is based on the Strang splitting procedure. Our approach combines the barycentric Lagrange interpolation collocation method for spatial approximation and a second-order Crank–Nicolson scheme for temporal approximation.

First, rewrite Equation (1) as follows,

$$iu_t=L(u)+N(u), \tag{22}$$

where $L(u)=-\rho\Delta u$ and $N(u)=-v(\mathbf{x})u-\beta|u|^2u$.

Then, Equation (1) is split into the linear part,

$$iu_t=L(u)=-\rho\Delta u, \tag{23}$$

and the nonlinear part,

$$iu_t=N(u)=-v(\mathbf{x})u-\beta|u|^2u. \tag{24}$$

Next, for a given time step, τ, the solution of Equation (1) evolves from t to $t+\tau$ via the Strang splitting method [23], which consists of three substeps:

$$u(x,y,t+\tau)=S^B(\frac{\tau}{2})S^A(\tau)S^B(\frac{\tau}{2})u(x,y,t)+O(\tau^3), \tag{25}$$

where S^A and S^B are the exact solution operators of Equation (23) and Equation (24), respectively.

Then, we will provide numerical approximations S_h^A and S_h^B for the exact solution operators S^A and S^B, respectively. Suppose $\Omega = [a,b] \times [c,d]$ and $\Omega_h = \{(x_i, y_j), i = 0 < 1 < \ldots < m, j = 0 < 1 < \ldots < n\}$. Here, x_i and y_j are Chebyshev mesh points.

To solve Equation (23), the barycentric Lagrange interpolation collocation method is applied to discretize the spatial derivative. The semi-discretized scheme in space is obtained based on the barycentric Lagrange interpolation collocation method, as introduced in Section 2.

$$iu_t(x_i, y_j, t) = -\rho \sum_{i=0}^{m} \sum_{j=0}^{n} \Big(\alpha_i''(x)\beta_j(y) + \alpha_i(x)\beta_j''(y)\Big) u(x_i, y_j, t). \tag{26}$$

The matrix form of (26) can be expressed as

$$i(u_h(t))_t = -\rho \Big(P^{(2)} \otimes I_n + I_m \otimes Q^{(2)}\Big) u_h(t), \tag{27}$$

where $u_h(t) = [u_{00}(t), \cdots, u_{0n}(t), u_{10}(t), \cdots, u_{1n}(t), \cdots, u_{m0}(t), \cdots, u_{mn}(t)]$, $u_{ij}(t) = u(x_i, y_j, t)$; $P^{(2)}$ and $Q^{(2)}$ are second-order differentiation matrices on nodes $x_0, x_1, \ldots, x_m$ and $y_0, y_1, \ldots, y_n$, respectively; $\otimes$ represents the Kronecker product of the matrix; I_m and I_n are the identity matrices of $m+1$ and $n+1$ order, respectively. Then, setting $u_h^k = u_h(t_k)$, we can obtain the following fully discretized scheme:

$$i\frac{u_h^{k+1} - u_h^k}{\tau} = -\rho(\frac{1}{2}(P^{(2)} \otimes I_n + I_m \otimes Q^{(2)})u_h^{k+1} + \frac{1}{2}(P^{(2)} \otimes I_n + I_m \otimes Q^{(2)})u_h^k). \tag{28}$$

Therefore, we obtain

$$S_h^A: \quad u_h^{k+1} = (iI + \frac{\rho\tau}{2}W)^{-1}(iI - \frac{\rho\tau}{2}W)u_h^k, \tag{29}$$

where I is the identity matrix of order $(m+1)(n+1)$, $W = P^{(2)} \otimes I_n + I_m \otimes Q^{(2)}$.

Then, Equation (24) can be solved analytically by

$$S_h^B: \quad u_h^{k+1} = e^{i\frac{\tau}{2}(v(x,y)+\beta|u_h^k|^2)}u_h^k. \tag{30}$$

The second-order operator splitting scheme can be derived as follows:

$$\textbf{MI:}\begin{cases} u_h^{(1)} = e^{i\frac{\tau}{2}(v(x,y)+\beta|u_h^k|^2)}u_h^k \\ u_h^{(2)} = (iI + \frac{\rho\tau}{2}W)^{-1}(iI - \frac{\rho\tau}{2}W)u_h^{(1)} \\ u_h^{k+1} = e^{i\frac{\tau}{2}(v(x,y)+\beta|u_h^{(2)}|^2)}u_h^{(2)} \end{cases}. \tag{31}$$

4. Convergence Analysis

Firstly, in this section we analyze the consistency of the semi-discretized scheme (26). Suppose that $q(x,y)$ is the Lagrange interpolation function of $u(x,y)$, satisfying $q(x_i, y_j) = u(x_i, y_j), i = 0 < 1 < \ldots < m, j = 0 < 1 < \ldots < n$.

By defining

$$r(x,y) = u(x,y) - q(x,y), \tag{32}$$

we can obtain the following estimates [18],

Lemma 1. *Suppose $u(x,y) \in C^{(\tilde{m}+1)}([a,b]\times[c,d])$, where $\tilde{m} = \max\{m,n\}$, we have*

$$\begin{cases} \|r(x,y)\|_\infty \le C_1 \parallel u^{(m+1)} \parallel_\infty \left(\frac{eh_x}{2m}\right)^m + C_2 \parallel u^{(m+1)} \parallel_\infty \left(\frac{eh_y}{2n}\right)^n \\ \|r_{xx}(x,y)\|_\infty \le C_1^{**}\|u^{(m+1)}\|_\infty \left(\frac{eh_x}{2(m-2)}\right)^{m-2} + C_2\|u^{(n+1)}\|_\infty \left(\frac{eh_y}{2n}\right)^n \\ \|r_{yy}(x,y)\|_\infty \le C_1\|u^{(m+1)}\|_\infty \left(\frac{eh_x}{2m}\right)^m + C_2^{**}\|u^{(n+1)}\|_\infty \left(\frac{eh_y}{2(n-2)}\right)^{n-2} \end{cases},$$

where $h_x = \frac{b-a}{2}$, $h_y = \frac{d-c}{2}$, and e is the natural constant.

Let $u(x,y,t)$ be the solution of Equation (1) and $u(x_i,y_j,t)$ is the numerical solution of $u(x,y,t)$ discretized by barycentric Lagrange interpolation collocation method; we then have

$$\mathcal{T}u(x_i,y_j,t) = 0 \tag{33}$$

and

$$\lim_{i,j\to\infty} \mathcal{T}u(x_i,y_j,t) = 0, \tag{34}$$

where $\mathcal{T} = i\dfrac{\partial}{\partial t} + \dfrac{\partial^2}{\partial x^2} + \dfrac{\partial^2}{\partial y^2}$.

Based on the above results, we obtain the following theorem.

Theorem 1. *Let $u(x_i,y_j,t) : \mathcal{T}u(x_i,y_j,t) = 0$, we have*

$$\|u(x,y,t) - u(x_i,y_j,t)\|_\infty \le C_1^{**} \parallel u^{(m+1)}\|_\infty \left(\frac{eh_x}{2(m-2)}\right)^{m-2} + C_2^{**} \parallel u^{(n+1)}\|_\infty \left(\frac{eh_y}{2(n-2)}\right)^{n-2}.$$

Proof. As

$$\begin{aligned} &\mathcal{T}u(x,y,t) - \mathcal{T}u(x_i,y_j,t) \\ &= iu_t(x,y,t) + u_{xx}(x,y,t) + u_{yy}(x,y,t) - \left(iu_t(x_i,y_j,t) + u_{xx}(x_i,y_j,t) + u_{yy}(x_i,y_j,t)\right) \\ &= iu_t(x,y,t) - iu_t(x_i,y_j,t) + u_{xx}(x,y,t) - u_{xx}(x_i,y_j,t) + u_{yy}(x,y,t) - u_{yy}(x_i,y_j,t) \\ &:= A_1 + A_2 + A_3, \end{aligned} \tag{35}$$

where A_1, A_2 and A_3 represent

$$\begin{aligned} A_1 &= iu_t(x,y,t) - iu_t(x_i,y_j,t), \\ A_2 &= u_{xx}(x,y,t) - u_{xx}(x_i,y_j,t), \\ A_3 &= u_{yy}(x,y,t) - u_{yy}(x_i,y_j,t). \end{aligned} \tag{36}$$

For A_1, we obtain

$$\begin{aligned} A_1 &= i(u_t(x,y,t) - u_t(x_i,y_j,t)) \\ &= i(u_t(x,y,t) - u_t(x_i,y,t) + u_t(x_i,y,t) - u_t(x_i,y_j,t)) \\ &= i(r_t(x_i,y,t) + r_t(x_i,y_j,t)). \end{aligned} \tag{37}$$

From Lemma 1, we can derive

$$\begin{aligned} &\|A_1\|_\infty = \|i(r_t(x_i,y,t) + r_t(x_i,y_j,t))\|_\infty \\ &\le \|r_t(x_i,y,t)\|_\infty + \|r_t(x_i,y_j,t)\|_\infty \\ &\le C_1 \parallel u^{(m+1)}\|_\infty \left(\frac{eh_x}{2m}\right)^m + C_2 \parallel u^{(n+1)}\|_\infty \left(\frac{eh_y}{2n}\right)^n. \end{aligned} \tag{38}$$

Similar estimates can be derived as follow:

$$\begin{aligned} \|A_2\|_\infty &= \|r_{xx}(x_i, y, t) + r_{xx}(x_i, y_j, t)\|_\infty \\ &\leq C_1^{**} \parallel u^{(m+1)} \|_\infty \left(\frac{eh_x}{2(m-2)}\right)^{m-2} + C_2 \parallel u^{(n+1)} \|_\infty \left(\frac{eh_y}{2n}\right)^{n}, \end{aligned} \tag{39}$$

$$\begin{aligned} \|A_3\|_\infty &= \|r_{yy}(x_i, y, t) + r_{yy}(x_i, y_j, t)\|_\infty \\ &\leq C_1 \parallel u^{(m+1)} \|_\infty \left(\frac{eh_x}{2m}\right)^{m} + C_2^{**} \parallel u^{(n+1)} \|_\infty \left(\frac{eh_y}{2(n-2)}\right)^{n-2}. \end{aligned} \tag{40}$$

From (38)–(40) and (35), the proof is completed. □

Next, we consider consistency analysis of the full-discretized scheme (28).

Theorem 2. *Suppose $u(x, y, t) \in C^{(\tilde{m}+1)}(\Omega) \times C^2(0, T], \Omega = [a, b] \times [c, d]$, where $\tilde{m} = \max\{m, n\}$ and $u(x_i, y_j, t_{k+1})$ is the corresponding numerical solution of $u(x, y, t)$, we have*

$$\|u(x, y, t) - u(x_i, y_j, t_{k+1})\|_\infty \leq C_3 \left(\tau^3 + \parallel u^{(m+1)} \|_\infty \left(\frac{eh_x}{2(m-2)}\right)^{m-2} + \parallel u^{(n+1)} \|_\infty \left(\frac{eh_y}{2(n-2)}\right)^{n-2}\right),$$

where C_3 is a positive constant.

Proof. Let $u(x, y, t_{k+1})$ be the corresponding numerical solution using the Crank–Nicolson scheme for temporal approximation of $u(x, y, t)$; we can obtain

$$i\delta u_t(x, y, t_{k+\frac{1}{2}}) = -\rho\Delta u(x, y, t_{k+\frac{1}{2}}) + R^k, \tag{41}$$

where $\delta u_t(x, y, t_{k+\frac{1}{2}}) = u(x, y, t_{k+1}) - u(x, y, t_k)$, and $R^k = u_t(x, y, t_{k+\frac{1}{2}}) - \delta u_t(x, y, t_{k+\frac{1}{2}})$ is the truncation error in time. Based on the principle of Taylor expansion, we can obtain

$$\left|R^k\right| \leq C_4\tau^3. \tag{42}$$

Equation (41) is discretized by the BLIC scheme, and supposing that $u(x_i, y_j, t_{k+1})$ is the numerical solution of $u(x, y, t_{k+1})$ based on the BLIC method, it holds that

$$i\delta u_t(x_i, y_j, t_{k+\frac{1}{2}}) = -\rho\Delta u^h(x_i, y_j, t_{k+\frac{1}{2}}) + R^k + \gamma^{i,j}, \tag{43}$$

where $\gamma^{i,j}$ represents the truncation error in space.

Combining Equations (41) and (43), we have

$$i\delta u_t(x, y, t_{k+\frac{1}{2}}) - i\delta u_t(x_i, y_j, t_{k+\frac{1}{2}}) = -\rho\Delta u(x, y, t_{k+\frac{1}{2}}) + \rho\Delta u^h(x_i, y_j, t_{k+\frac{1}{2}}) - \gamma^{i,j}. \tag{44}$$

If we use a similar technique in Theorem 1, we can derive

$$\left|\gamma^{i,j}\right| \leq C_1^{**} \parallel u^{(m+1)} \|_\infty \left(\frac{eh_x}{2(m-2)}\right)^{m-2} + C_2^{**} \parallel u^{(n+1)} \|_\infty \left(\frac{eh_y}{2(n-2)}\right)^{n-2}. \tag{45}$$

Combining (42) and (45), the proof is completed. □

We will now analyze the error results of the operator splitting scheme.

Define a grid function space on Ω_h,

$$\mathcal{W}^h = \left\{U \middle| U = \{U_{ij} \mid 0 \leq i \leq m, 0 \leq j \leq n\}\right\},$$

and a mapping $I^h : \tilde{H}(\Omega) \longrightarrow \mathcal{W}_h$ by

$$I^h(u) = U,$$

where $\tilde{H}(\Omega) = \{u \in H^2(\Omega) \mid u(\mathbf{x}, t) = 0\}$.

Lemma 2. *Supposing that $U \in \mathcal{W}^h$, $\|W\|_\infty$ is bounded and τ is small enough, we have*

$$\| S_h^A(\tau)U \|_\infty \leq (1 + \kappa\tau) \| U \|_\infty .$$

Proof. By Taylor expansion, the approximation of $(iI + \frac{\rho\tau}{2}W)^{-1}$ at the zero matrix is

$$(iI + \frac{\rho\tau}{2}W)^{-1} = -iI + \frac{\rho\tau}{2}W + i\frac{(\rho\tau)^2}{4}W^2 - \frac{(\rho\tau)^3}{8}W^3 + \mathcal{O}(\tau^4). \tag{46}$$

Then, combining with the above formula, we can obtain

$$\| (iI + \frac{\rho\tau}{2}W)^{-1}(iI - \frac{\rho\tau}{2}W)\|_\infty = \| I + i\rho\tau W - \frac{(\rho\tau)^2}{2}W^2 - \frac{(\rho\tau)^4}{16}W^4\|_\infty \leq 1 + \kappa\tau. \tag{47}$$

Therefore,

$$\begin{aligned} &\| S_h^A(\tau)U\|_\infty = \| (iI + \frac{\rho\tau}{2}W)^{-1}(iI + \frac{\rho\tau}{2}W)U\|_\infty \\ &\leq \| (iI + \frac{\rho\tau}{2}W)^{-1}(I + \frac{\rho\tau}{2}W)\|_\infty \| U\|_\infty \\ &\leq (1 + \kappa\tau) \| U\|_\infty \end{aligned}, \tag{48}$$

where κ is a positive constant independent of τ. □

Lemma 3. *Supposing that $U \in \mathcal{W}^h$, we have*

$$\| S_h^B(\frac{\tau}{2})U \|_\infty = \| U \|_\infty .$$

Proof.

$$\left|S_h^B(\frac{\tau}{2})u_{ij}\right| = \left|e^{i\frac{\tau}{2}(v(x,y)+\beta|u_{ij}|^2)}\right|\left|u_{ij}\right| = \left|u_{ij}\right|. \tag{49}$$

□

By Theorem 2, we can obtain the following result.

Lemma 4. *Supposing that $u_0 \in \tilde{H}(\Omega)$, we have*

$$\| I^h S^A u_0 - S_h^A I^h u_0 \|_\infty \leq C_1^{**} \| u^{(m+1)}\|_\infty \left(\frac{eh_x}{2(m-2)}\right)^{m-2} + C_2^{**} \| u^{(n+1)}\|_\infty \left(\frac{eh_y}{2(n-2)}\right)^{n-2} + C_4\tau^3.$$

For convenience, suppose

$$\eta = C_5\left(\| u^{(m+1)}\|_\infty \left(\frac{eh_x}{2(m-2)}\right)^{m-2} + \| u^{(n+1)}\|_\infty \left(\frac{eh_y}{2(n-2)}\right)^{n-2} + \tau^3\right),$$

where $C_5 = \max\{C_1^{**}, C_2^{**}, C_4\}$.

Theorem 3. *Let $u^{k+1} \in \tilde{H}(\Omega)$ be the exact solution of Equation (1) and $\tilde{u}(x, y, t)$ and U^{k+1} be the exact solution of Equation (25) and the numerical solution at t_{k+1} of Equation (31), respectively. According to Theorem 1 and Lemma 2, we have*

$$\| I^h u^{k+1} - U^{k+1} \|_\infty \leq C\left(\frac{\| u^{(m+1)}\|_\infty}{\tau}\left(\frac{eh_x}{2(m-2)}\right)^{m-2} + \frac{\| u^{(n+1)}\|_\infty}{\tau}\left(\frac{eh_y}{2(n-2)}\right)^{n-2} + \tau^2\right),$$

where C is a positive constant independent of τ.

Proof. For $k \geq 0$, we obtain

$$\| I^h u^{k+1} - U^{k+1} \|_\infty \leq \| I^h u^{k+1} - I^h \tilde{u}^{k+1} \|_\infty + \| I^h \tilde{u}^{k+1} - U^{k+1} \|_\infty . \tag{50}$$

From [23], we obtain

$$\| I^h \tilde{u}^{k+1} - I^h u^{k+1} \|_\infty \leq C_6 \tau^2. \tag{51}$$

By Lemma 3, we obtain

$$\begin{aligned} &\| I^h \tilde{u}^{k+1} - U^{k+1} \|_\infty \\ &= \| I^h S^B S^A S^B \tilde{u}^k - S_h^B S_h^A S_h^B U^k \|_\infty \\ &\leq \| I^h S^B S^A S^B \tilde{u}^k - S_h^B I^h S^A S^B \tilde{u}^k \|_\infty + \| S_h^B I^h S^A S^B \tilde{u}^k - S_h^B S_h^A S_h^B U^k \|_\infty \\ &\leq \| I^h S^A S^B \tilde{u}^k - S_h^A S_h^B U^k \|_\infty \end{aligned}. \tag{52}$$

From Lemmas 2 and 4, we obtain

$$\begin{aligned} &\| I^h S^A S^B \tilde{u}^k - S_h^A S_h^B U^k \|_\infty \\ &\leq \| I^h S^A S^B \tilde{u}^k - S_h^A I^h S^B \tilde{u}^k \|_\infty + \| S_h^A I^h S^B \tilde{u}^k - S_h^A S_h^B U^k \|_\infty. \\ &\leq \eta + (1+\kappa\tau) \| I^h S^B \tilde{u}^k - S_h^B U^k \|_\infty \end{aligned} \tag{53}$$

From Lemma 3, we derive

$$\begin{aligned} &\| I^h S^B \tilde{u}^k - S_h^B U^k \|_\infty \\ &\leq \| I^h S^B \tilde{u}^k - S_h^B I^h \tilde{u}^k \|_\infty + \| S_h^B I^h \tilde{u}^k - S_h^B U^k \|_\infty. \\ &\leq \| I^h \tilde{u}^k - U^k \|_\infty \end{aligned} \tag{54}$$

Due to $\| I^h \tilde{u}^0 - U^0 \|_\infty = 0$, and by the Gronwall inequality, we can obtain

$$\begin{aligned} &\| I^h \tilde{u}^{k+1} - U^{k+1} \|_\infty \\ &\leq \eta + (1+\kappa\tau) \| I^h \tilde{u}^k - U^k \|_\infty \\ &\leq \sum_{j=0}^{k} (1+\kappa\tau)^j \eta + (1+\kappa\tau)^{k+1} \| I^h \tilde{u}^0 - U^0 \|_\infty \\ &\leq \frac{(1+\kappa\tau)^{k+1} - 1}{1+\kappa\tau - 1}\eta \\ &\leq \frac{e^{\kappa\tau}}{\kappa\tau}\eta \end{aligned}. \tag{55}$$

By the above estimates and the expression of η, we have

$$\begin{aligned} &\| I^h u^{k+1} - U^{k+1} \|_\infty \\ &\leq \frac{e^{\kappa\tau}}{\kappa}\left(C_5\left(\frac{\| u^{(m+1)}\|_\infty}{\tau}\left(\frac{eh_x}{2(m-2)}\right)^{m-2} + \frac{\| u^{(n+1)}\|_\infty}{\tau}\left(\frac{eh_y}{2(n-2)}\right)^{n-2} + \tau^2\right)\right), \\ &\leq C\left(\frac{\| u^{(m+1)}\|_\infty}{\tau}\left(\frac{eh_x}{2(m-2)}\right)^{m-2} + \frac{\| u^{(n+1)}\|_\infty}{\tau}\left(\frac{eh_y}{2(n-2)}\right)^{n-2} + \tau^2\right) \end{aligned} \tag{56}$$

where $C = \max\left\{C_5\frac{e^{\kappa\tau}}{\kappa}, C_5\frac{e^{\kappa\tau}}{\kappa} + C_6\right\}$. The proof is completed. □

5. Numerical Experiments

In this section, we will provide some numerical results for the NLS Equation (1) to test the high accuracy and efficiency of our scheme. For convenience, the error notations are given as follows,

$$E_\infty = \| u_h - u_e \|_\infty, \tag{57}$$

$$E_r = \frac{\| u_h - u_e \|_\infty}{\| u_e \|_\infty}, \tag{58}$$

where u_h and u_e denote the numerical solution and the exact solution, respectively. $\| \cdot \|_\infty$ is the L^∞ norm. All computations presented in this work were performed on a standard i5 Intel 1.8GHz laptop in MATLAB R2020b.

5.1. Example 1

This example is used to test the accuracy and convergence of our scheme. Considering the following 2D NLS equation on $[0, 2\pi]^2 \times (0, T]$,

$$\begin{cases} iu_t + \frac{1}{2}\Delta u - (1 - \sin^2 x \sin^2 y)u - |u|^2 u = 0 \\ u(x, y, 0) = \sin x \sin y \\ u(0, y, t) = u(2\pi, y, t) = 0 \\ u(x, 0, t) = u(x, 2\pi, t) = 0 \end{cases},$$

where the exact solution is in the following form:

$$u(x, y, t) = e^{-2it} \sin x \sin y.$$

To verify the accuracy and the convergence rate of the operator splitting scheme based on the barycentric Lagrange interpolation collocation method **MI**, the operator splitting scheme based on the barycentric rational interpolation collocation method [24] **MII** and the classical second-order finite difference scheme **SI**, we choose the simulation parameters $n = m$, $\tau = 0.001$ and $T = 1$.

The results are shown in Tables 1–4 and Figures 1–3. Tables 1–3 show the spatial errors of the three schemes. By comparing Tables 1 and 3, it can be seen that the **MI** scheme, based on the barycentric Lagrange interpolation collocation method in space, can achieve a higher accuracy using only 8×8 mesh points. However, for the same accuracy, the **SI** scheme, based on a second-order center difference method in space, requires more than 80×80 mesh points. Furthermore, by comparing Tables 1 and 2, it is easy to see that the **MI** scheme is slightly more efficient than the **MII** scheme. The comparison of the three schemes shows that the barycentric Lagrange interpolation collocation scheme can achieve higher accuracy with fewer points in space. In addition, the CPU time of the **MI** scheme is significantly reduced compared with the **SI** scheme and is similar to the **MII** scheme.

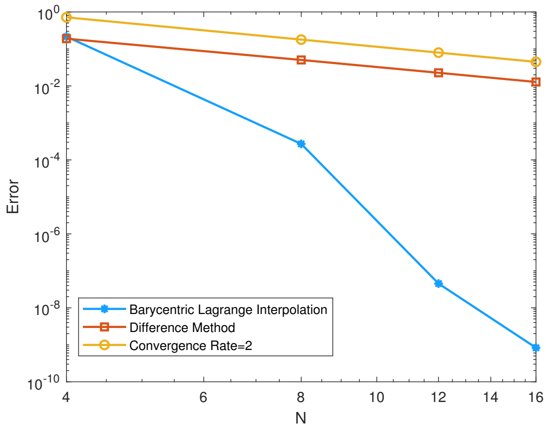

Figure 1. Spatial L^{∞} errors at $t = 1$ for NLS equation for Example 1.

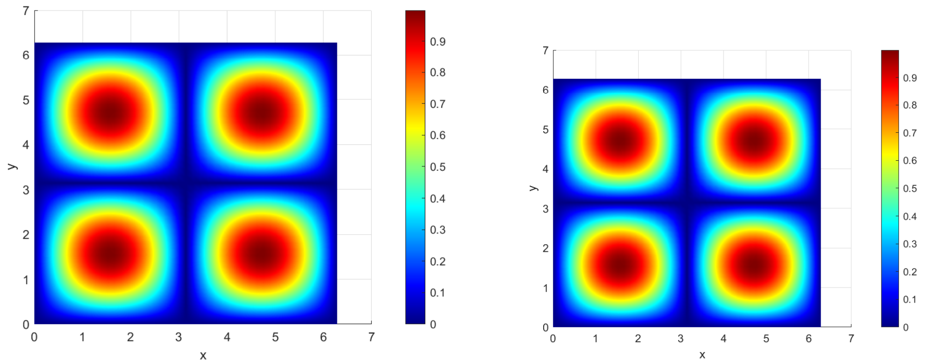

(**a**) The numerical solution diagram (**b**) The exact solution diagram

Figure 2. The numerical solution and the exact solution diagrams at $T = 1$ for Example 1.

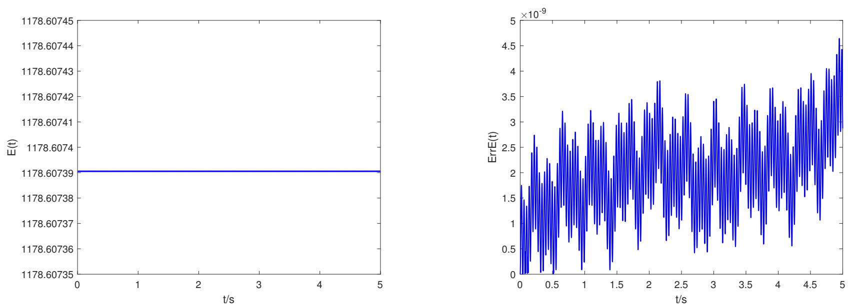

(**a**) Total energy (**b**) Energy relative error

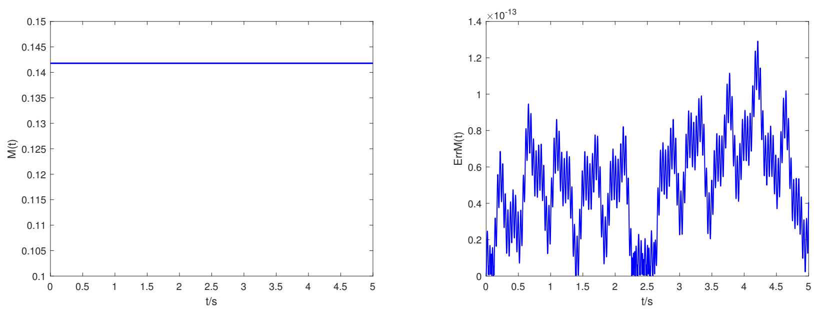

(**c**) Total mass (**d**) Mass relative error

Figure 3. Conservation situation of energy and mass at $T = 1$ for Example 1.

Table 1. Error of barycentric Lagrange interpolation collocation scheme for Example 1.

m	E_∞	E_r	*CPU*
6	8.4010×10^{-3}	8.4010×10^{-3}	0.152 s
8	2.3542×10^{-4}	2.7054×10^{-4}	0.288 s
10	1.9318×10^{-6}	2.0865×10^{-6}	0.694 s
12	5.6755×10^{-8}	5.6755×10^{-8}	1.039 s
16	8.0816×10^{-8}	8.3330×10^{-8}	2.914 s

Table 2. Error of barycentric rational interpolation collocation method for Example 1.

m	E_∞	E_r	*CPU*
6	2.9302×10^{-3}	2.9302×10^{-3}	0.178 s
8	2.7122×10^{-3}	3.1167×10^{-3}	0.289 s
10	5.4257×10^{-6}	5.8602×10^{-6}	0.735 s
12	2.0948×10^{-6}	2.0948×10^{-6}	1.082 s
16	8.3994×10^{-8}	8.6607×10^{-8}	3.066 s

Table 3. Error of difference scheme for Example 1.

m	E_∞	E_r	*CPU*
10	2.9367×10^{-2}	3.2467×10^{-2}	0.202 s
20	8.1977×10^{-3}	8.1977×10^{-3}	3.586 s
40	2.0546×10^{-3}	2.0546×10^{-3}	160.534 s
60	9.1360×10^{-4}	9.1360×10^{-4}	1665.769 s
80	5.1402×10^{-4}	5.1402×10^{-4}	8993.522 s

Table 4. Errors and convergence rate in time for Example 1.

τ	E_∞	*Rate*	E_r	*Rate*
1/8	1.2598×10^{-3}	-	1.2990×10^{-3}	-
1/16	3.1552×10^{-4}	1.9975	3.2533×10^{-4}	1.9975
1/32	7.8913×10^{-5}	1.9994	8.1368×10^{-5}	1.9994
1/64	1.9731×10^{-5}	1.9998	2.0344×10^{-5}	1.9998

If we fix $m = n = 16$ and vary the temporal step, τ, we can obtain errors and temporal convergence rate, as shown in Table 2. It shows that the **MI** scheme based on the barycentric interpolation collocation scheme for the NLS equation has second-order accuracy in time. In addition, the spatial convergence rate is also obtained, and the L^∞ errors at time $T = 1$ for NLS equation are shown in Figure 1.

Choose $m = n = 20$; the numerical solution and the exact solution of the NLS equation are shown in Figure 2a,b. Moreover, it is necessary to verify the conservation of energy and mass. We plot images of mass and energy varying over time. From Figure 3, it is obvious that mass and energy are conserved.

5.2. Example 2

Consider the following 1D problem on $[-10, 40] \times (0, 9]$:

$$\begin{cases} iu_t + \Delta u + 2|u|^2 u = 0, \\ u(-10, t) = u(40, t) = 0, \\ u_0(x) = \operatorname{sech}(x)\exp(2ix) + \operatorname{sech}(x-30)\exp(-i(x-30)). \end{cases}$$

This example shows the collision behavior of two solitary waves. If we provide the initial value condition, a double solitary wave can be generated. When $t = 0$, two solitary waves are separated. The fast wave will catch up with the slow wave over time, and it will then surpass the slow wave after the collision, and there is only one phase change between them. This is consistent with the theory of waves; see Figures 4 and 5.

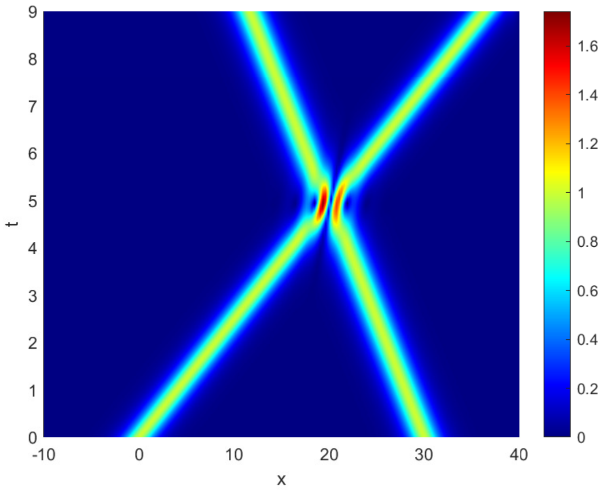

Figure 4. The interaction of two solitary waves without damping at $T = 9$ for Example 2.

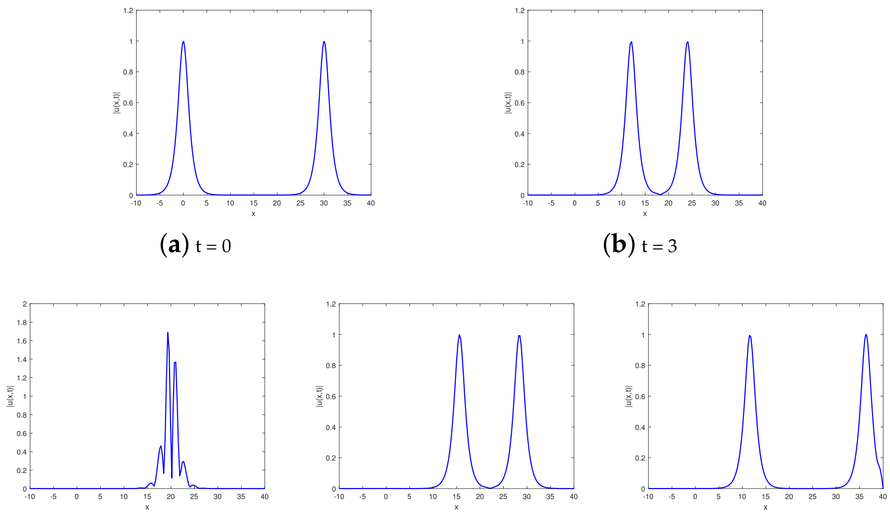

(**a**) t = 0 (**b**) t = 3

(**c**) t = 5 (**d**) t = 7 (**e**) t = 9

Figure 5. Head-on collisions of two solitary waves without damping for Example 2.

6. Conclusions

In this work, we have proposed an effective operator splitting scheme based on the barycentric Lagrange interpolation collocation method for the nonlinear Schrödinger equation. The convergence analysis is proved theoretically and verified numerically. Numerical examples are presented to show the mass and energy conservation of the proposed scheme. The operator splitting collocation scheme is second-order in time and convergent exponentially in space. The two barycentric interpolation collocation schemes have high accuracy, and the barycentric Lagrange interpolation collocation method is slightly more efficient than the barycentric rational interpolation collocation method. Compared with the finite difference method, the barycentric interpolation collocation method can achieve high accuracy with fewer points. In the future, we plan to extend this method to coupled Schrödinger equations, KdV equations and Klein–Gordon equations, etc.

Author Contributions: M.Y., methodology, conceptualization, design, analysis, software, original draft writing; Z.W., methodology, supervision, conceptualization, editing, draft editing and reviewing. All authors have read and agreed to the published version of the manuscript.

Funding: The research was funded by the Natural Science Foundation of Fujian Province (Nos. 2022J01308, 2021J01306), the NSF of China (No. 11701197), the Program for Innovative Research Teams in Science and Technology in Fujian Province University and the Fuzhou-Xiamen-Quanzhou National Independent Innovation Demonstration Zone Collaborative Innovation Platform under Grant 2022FX5.

Data Availability Statement: No new data were created or analyzed in this study.

Acknowledgments: We thank the anonymous referees for their careful checking and valuable comments which improve the manuscript.

Conflicts of Interest: The authors declare no conflicts of interest.

References

1. Schrödinger, E. The present status of quantum mechanics. *Sci. Nat.* **1935**, *23*, 1–26.
2. Gong, Y.Z.; Wang, Q.; Wang, Y.S.; Cai, J.X. A conservative Fourier pseudo-spectral method for the nonlinear Schrödinger equation. *J. Comput. Phys.* **2017**, *328*, 354–370. [CrossRef]
3. Cui, J.; Xu, Z.Z.; Wang, Y.S.; Jiang, C.L. Mass-and energy-preserving exponential Runge–Kutta methods for the nonlinear Schrödinger equation. *Appl. Math. Lett.* **2020**, *112*, 106770. [CrossRef]
4. Feng, X.B.; Li, B.Y.; Ma, S. High-order mass-and energy-conserving SAV-Gauss collocation finite element methods for the nonlinear Schrödinger equation. *SIAM J. Numer. Anal.* **2021**, *59*, 1566–1591. [CrossRef]
5. Wang, J.J.; Li, M.; Guo, L.J. Superconvergence analysis for nonlinear Schrödinger equation with two-grid finite element method. *Appl. Math. Lett.* **2021**, *122*, 107553. [CrossRef]
6. Wang, L.L.; Li, M. Galerkin finite element method for damped nonlinear Schrödinger equation. *Appl. Numer. Math.* **2022**, *178*, 216–247. [CrossRef]
7. Hu, H.Z.; Li, B.Y.; Zou, J. Optimal convergence of the Newton iterative Crank–Nicolson finite element method for the nonlinear Schrödinger equation. *Comput. Methods Appl. Math.* **2022**, *22*, 91–612. [CrossRef]
8. Chen, C.J.; Lou, Y.Z.; Hu, H.Z. Two-grid finite volume element method for the time-dependent Schrödinger equation. *Comput. Math. Appl.* **2022**, *108*, 185–195. [CrossRef]
9. Deng, B.C.; Shen, J.; Zhuang, Q.Q. Second-order SAV schemes for the nonlinear Schrödinger equation and their error analysis. *J. Sci. Comput.* **2021**, *69*, 88. [CrossRef]
10. Su, C.M.; Zhao, X.F. On time-splitting methods for nonlinear Schrödinger equation with highly oscillatory potential. *Math. Model. Numer. Anal.* **2020**, *54*, 1491–1508. [CrossRef]
11. Wang, T.C.; Zhao, X.F. Optimal L^∞ error estimates of finite difference methods for the coupled Gross–Pitaevskii equations in high dimensions. *Sci. China Math.* **2014**, *57*, 2189–2214. [CrossRef]
12. Li, J.; Qu, J.Z. Barycentric Lagrange interpolation collocation method for solving the Sine-Gordon equation. *Wave Motion* **2023**, *120*, 103159. [CrossRef]
13. Hu, Y.D.; Peng, A.; Chen, L.Q.; Tong, Y.L.; Weng, Z.F. Analysis of the barycentric interpolation collocation scheme for the Burgers equation. *Sci. Asia* **2021**, *47*, 758–765. [CrossRef]
14. Oruç, Ö. Two meshless methods based on local radial basis function and barycentric rational interpolation for solving 2D viscoelastic wave equation. *Comput. Appl. Math.* **2020**, *79*, 3272–3288. [CrossRef]
15. Deng, Y.F.; Weng, Z.F. Barycentric interpolation collocation method based on Crank–Nicolson scheme for the Allen–Cahn equation. *AIMS Math.* **2021**, *6*, 3857–3873. [CrossRef]
16. Deng,Y.F.; Weng, Z.F. Operator splitting scheme based on barycentric Lagrange interpolation collocation method for the Allen–Cahn equation. *J. Appl. Math. Comput.* **2022**, *68*, 3347–3365. [CrossRef]
17. Huang, R.; Weng, Z.F. A numerical method based on barycentric interpolation collocation for nonlinear convection-diffusion optimal control problems. *Netw. Heterog. Media* **2023**, *18*, 562–580. [CrossRef]
18. Yi, S.C.; Yao, L.Q. A steady barycentric Lagrange interpolation method for the 2D higher-order time-fractional telegraph equation with nonlocal boundary condition with error analysis. *Numer. Methods Partial Differ. Equ.* **2019**, *35*, 1694–1716. [CrossRef]
19. Lubich, C. On splitting methods for Schrödinger–Poisson and cubic nonlinear Schrödinger equations. *Math. Comput.* **2008**, *77*, 2141–2153. [CrossRef]
20. Zhai, S.Y.; Wang, D.L.; Weng, Z.F.; Zhao, X. Error analysis and numerical simulations of Strang splitting method for space fractional nonlinear Schrödinger equation. *J. Sci. Comput.* **2019**, *81*, 965–989. [CrossRef]
21. Zhai, S.; Weng, Z.; Zhuang, Q.; Liu, F.; Anh, V. An effective operator splitting method based on spectral deferred correction for the fractional Gray–Scott model. *J. Comput. Appl. Math.* **2023**, *425*, 114959. [CrossRef]
22. Berrut, J.P.; Trefethen, L.N. Barycentric Lagrange interpolation. *SIAM Rev.* **2004**, *46*, 501–507. [CrossRef]

23. Strang, G. On the construction and comparison of difference schemes. *SIAM J. Numer. Anal.* **1968**, *5*, 506–517. [CrossRef]
24. Li, J.; Cheng, Y.L. Linear barycentric rational collocation method for solving heat conduction equation. *Numer. Methods Partial Differ. Equ.* **2021**, *37*, 533–545. [CrossRef]